Nonlinear detection of spin currents in graphene with non-magnetic electrodes

Vera-Marun, Ivan J.; Ranjan, Vishal; van Wees, Bart J.

Published in:
Nature Physics

DOI:
10.1038/NPHYS2219

Publication date:
2012

nature physics

SUPPLEMENTARY INFORMATION

DOI: 10.1038/NPHYS2219

Nonlinear detection of spin currents in graphene with non-magnetic electrodes

Ivan J. Vera-Marun,[a] Vishal Ranjan, and Bart J. van Wees

Physics of Nanodevices, Zernike Institute for Advanced Materials, University of Groningen, The Netherlands

SUPPLEMENTARY INFORMATION A

Here we present spin transport data acquired at liquid-nitrogen temperature (77 K). First, we show linear spin transport at 77 K and compare it with that at room temperature. Then we present partial data on non-linear spin detection using non-magnetic detectors at 77 K.

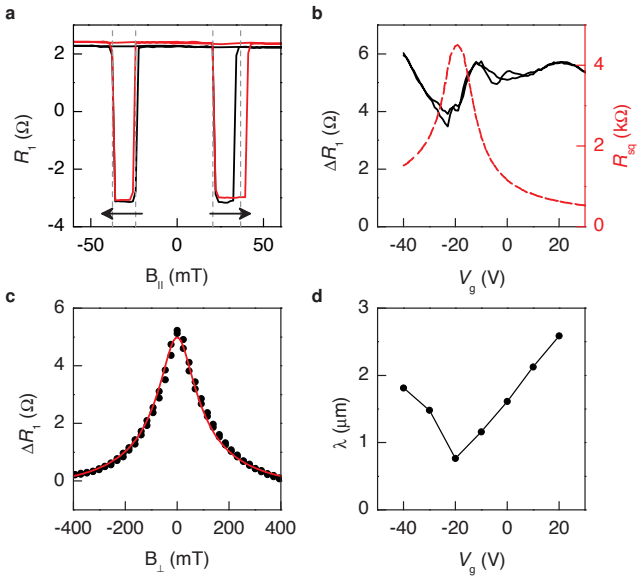

FIG. 1. **Linear spin detection using a magnetic detector at 77 K. a,** Two curves showing the spin-valve effect in non-local linear resistance R_1 by sweeping an in-plane magnetic field at $V_g = 0$ V. Two well-defined values correspond to parallel (R_1^{Pa}) and anti-parallel (R_1^{Ap}) alignment of Co contacts. **b,** Spin resistance $\Delta R_1 = R_1^{\mathrm{Pa}} - R_1^{\mathrm{Ap}}$ versus V_g. The dashed line is the square resistance R_{sq} of graphene between Contacts 2 and 3 with $V_D \approx -20$ V. **c,** Hanle spin precession curve by sweeping a perpendicular magnetic field at $V_g = 10$ V. The solid line is a fit with the one-dimensional Bloch equation. The obtained parameters are $D = 0.053\ \mathrm{m}^2/\mathrm{s}$ and $\tau = 86$ ps, with contact spin polarization $P = 7$ %. **d,** Spin relaxation length $\lambda = \sqrt{D\tau}$, with D and τ extracted from Hanle curves taken at several values of V_g.

We start by characterizing spin transport in the linear regime at 77 K. The results in Fig. 1 show a non-local spin-valve effect, again demonstrating spin transport between Contacts 2 and 3. The spin resistance is

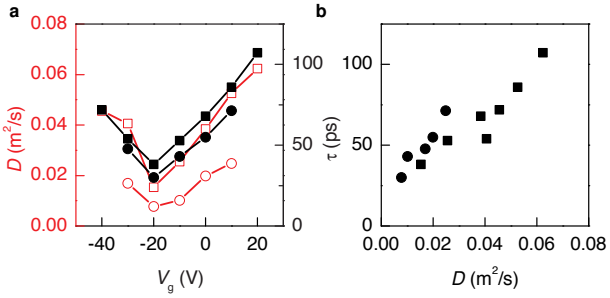

FIG. 2. **Comparison of spin transport parameters at 77 K and at room temperature. a,** Gate voltage dependence of the spin diffusion constant D (red open symbols) and the spin relaxation time (black closed symbols). **b,** Spin relaxation time versus spin diffusion constant. Data for both 77 K (squares) and room temperature (circles).

$\Delta R_1 \approx 5\ \Omega$ and shows a minimum close to the Dirac point. This result for ΔR_1 is similar to that at room temperature (shown in the main text) but ≈ 20 % larger. A larger ΔR_1 at 77 K can be understood from the analysis of Hanle spin precession curves (see Fig. 1c) from where we extract spin relaxation lengths ≈ 60 % larger than at room temperature. The effect of larger values of λ at 77 K is slightly compensated in our sample by a lower contact spin polarization $P = 7$ %.

The gate voltage dependence of the spin relaxation length $\lambda = \sqrt{\tau D}$ at 77 K (see Fig. 1d) shows a minimum close to the Dirac point, similar to the data at room temperature. This behavior is a result of the gate voltage dependence of D and τ, where both parameters show a minimum close to the Dirac point and exhibit a linear scaling $\tau \propto D$, as shown in Fig. 2. The latter is is indicative of the Elliot-Yafet mechanism of spin relaxation in single-layer graphene[1–3] being dominant both at room temperature and at 77 K.

Finally, in Fig. 3 we demonstrate non-linear detection of spins by using non-magnetic contacts at 77 K. Although our data at low temperature is limited, it shows a similar behavior of ΔR_2 as that at room temperature. The magnitude of ΔR_2 at both temperatures is similar within the experimental uncertainty, except for an almost 2 times higher value at $V_g = -10$ V close to the Dirac point. The observation of similar results at room temperature and at 77 K are a confirmation of our interpretation of the non-linear spin-valve signal as solely arising from an interaction between spin and charge, which does not directly involve heat as in the case of spin thermoelectric

[a]e-mail: I.J.Vera.Marun@rug.nl

DOI: 10.1038/NPHYS2219

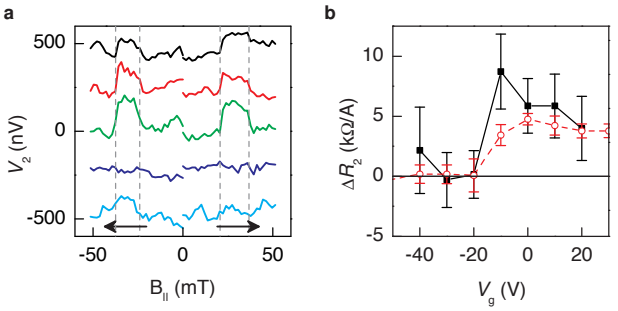

FIG. 3. **Non-linear spin detection using non-magnetic detectors at 77 K. a,** Second order signal showing spin-valve effect at 77 K. Two well-defined values correspond to parallel ($V_2^{\rm Pa}$) and anti-parallel ($V_2^{\rm Ap}$) alignment of the Co contacts. The curves correspond to (from top to bottom) $V_g = 20, 0, -10, -20$ and -40 V and are offset vertically for clarity. Each curve is the average of 26 measurements. All data for a root mean square current of 5 μA. **b,** Non-linear spin resistance $\Delta R_2 = R_2^{\rm Ap} - R_2^{\rm Pa}$ versus V_g at 77 K (closed black squares). For each data point the average value of V_2 for (anti)parallel configuration, and their standard deviation, was extracted from curves as those shown in **a**. The data for room temperature (open red circles) is also shown for comparison.

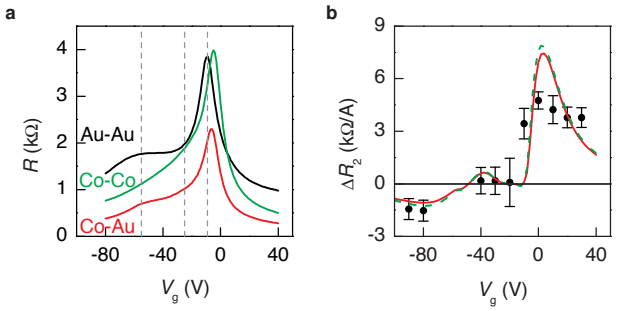

FIG. 4. **Effect of Co and Au contacts on graphene doping at room temperature. a,** Dirac curve of graphene between Contacts 2 and 3 (Co-Co, green), graphene between Contacts 3 and 4 (Co-Au, red) and graphene between Contacts 4 and 5 (Au-Au, black). Vertical dashed lines indicate the location of the Dirac point V_D for different graphene regions. **b,** Non-linear spin resistance $\Delta R_2 = R_2^{\rm Ap} - R_2^{\rm Pa}$ versus V_g. The red solid line is for the model described in the main text, considering graphene regions under both Au and Co contacts to behave the same with $V_D = -55$ V. The dashed green line is for considering graphene under the Co contacts to have a Dirac point $V_D = -20$ V. The data for room temperature (black circles) is also shown for comparison.

effects[4–6].

SUPPLEMENTARY INFORMATION B

Here we discuss on the identification of contributions to the Dirac curve from graphene regions under and around the contacts and those away from the contacts. We also discuss on the nature of the contacts and their possible contributions to the non-linear spin signal.

In the main text we showed how the Dirac curve for graphene between the two Au detectors is composed of two distinct contributions. The main contribution corresponds to regions of the graphene channel located away from the contacts, with a Dirac point $V_D = -9$ V. A minor contribution, visible as a kink in the hole regime[7], corresponds to regions of graphene located under (and next to) the Au contacts with $V_D = -55$ V (due to contact doping). We also observed similar kinks for the Dirac curves for graphene between the adjacent Co injector and Au detector, and for graphene between the two Co contacts used for spin injection (see Fig. 4a). The kinks in the Dirac curves indicate that the Co contacts also dope the graphene channel but with a Dirac point close to $V_D = -20$ V, different than for graphene around the Au contacts ($V_D = -55$ V).

The resulting ΔR_2 for the model presented in the main text corresponds to the simple case of assumption that all contacts have the same effect on graphene, with $V_D = -55$ V. In Fig. 4b we also show the result of incorporating in the model a different contribution from the Co contacts, with $V_D = -20$ V. Notice this consideration does not have a significant effect on the modelled ΔR_2. There are two reasons for this observation. First, the graphene regions modified by the presence of the Co contacts are not within the detector circuit. Therefore, charge potentials generated due to their α parameter have no influence on the signal detected between the Au contacts. Second, though the graphene regions under the Co contacts do have an influence on the $\Delta\mu$ profile via their resistivity (Dirac curve), this influence is small because these regions are narrow compared to the full extent of graphene over which $\Delta\mu$ decays. So the consideration of doping effects under the Co contacts is not critical for understanding the non-linear spin signal measured via the Au contacts.

A fundamental question is whether the contacts themselves contribute to the measured non-linear spin signal. This signal, generated via the non-linear interaction between spin and charge, relies on achieving a large enough $\Delta\mu$ and having a sizable α parameter. Owing to the large conductivity of metals, the achieved spin accumulation within the Au and Co metals (≈ 1 μeV)[8] is much lower than in graphene. So we do not expect a sizable signal coming from the bulk of the metallic contacts.

The discussion above leaves us with the final possibility that the graphene-metal interface could produce a sizable signal. Spin thermoelectric effects have been observed in high-quality tunnel contacts[6], as expected from the strong energy dependence of electron transmission through a tunnel barrier. To address this issue we have characterized the charge density and bias dependence of contact resistances in our device. From the results in Fig. 5 we observe that the contacts only change up to

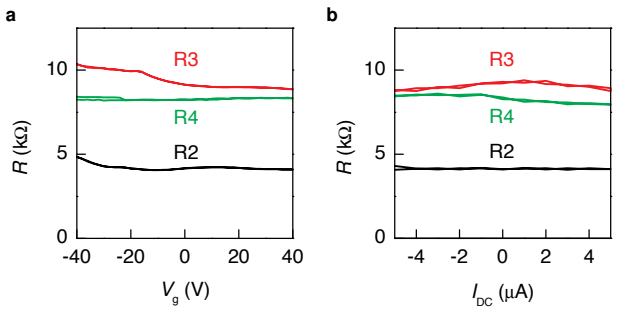

FIG. 5. **Contact characterization at 77 K. a,** Gate voltage dependence of resistances of Contacts 2, 3 and 4. Data for a root mean square current of 2 μA. **b,** Differential resistances of Contacts 2, 3 and 4 versus d.c. current bias, for a root mean square modulation of 0.1 μA.

20 % with gate voltage, and have linear $I-V$ characteristics (constant dV/dI within 10 % for the explored biasing currents). These contact characteristics have been previously observed on similar samples and were ascribed to transport dominated by relatively transparent regions in the oxide barrier[9]. In this case we do not expect that the interface would exhibit a sizable α parameter and its contribution to the non-linear spin signal would be negligible. We conclude the latter is applicable to our device, as we did not require to include this effect in our model in order to achieve a satisfactory description of the experimental data.

REFERENCES

[1] Józsa, C. *et al.* Linear scaling between momentum and spin scattering in graphene. *Phys. Rev. B* **80**, 241403(R) (2009).
[2] Avsar, A. *et al.* Toward wafer scale fabrication of graphene based spin valve devices. *Nano Lett.* **11**, 2363–2368 (2011).
[3] Han, W. & Kawakami, R. K. Spin relaxation in Single-Layer and bilayer graphene. *Phys. Rev. Lett.* **107**, 047207 (2011).
[4] Uchida, K. *et al.* Observation of the spin seebeck effect. *Nature* **455**, 778–781 (2008).
[5] Slachter, A., Bakker, F. L., Adam, J. & van Wees, B. J. Thermally driven spin injection from a ferromagnet into a non-magnetic metal. *Nature Phys.* **6**, 879–882 (2010).
[6] Le Breton, J., Sharma, S., Saito, H., Yuasa, S. & Jansen, R. Thermal spin current from a ferromagnet to silicon by seebeck spin tunnelling. *Nature* **475**, 82–85 (2011).
[7] Nouchi, R. & Tanigaki, K. Charge-density depinning at metal contacts of graphene field-effect transistors. *Appl. Phys. Lett.* **96**, 253503 (2010).
[8] Jedema, F. J., Filip, A. T. & van Wees, B. J. Electrical spin injection and accumulation at room temperature in an all-metal mesoscopic spin valve. *Nature* **410**, 345–348 (2001).
[9] Popinciuc, M. *et al.* Electronic spin transport in graphene field-effect transistors. *Phys. Rev. B* **80**, 214427 (2009).